

## Biocatalytic Conversion of Lignin to Aromatic Dicarboxylic Acids in *Rhodococcus jostii* RHA1 by Re-Routing Aromatic Degradation Pathways

Zoe Mycroft<sup>a</sup>, Maria Gomis<sup>b</sup>, Paul Mines<sup>b</sup>, Paul Law<sup>b</sup>, and Timothy D.H. Bugg<sup>a\*</sup>

<sup>a</sup>Department of Chemistry, University of Warwick, Coventry CV4 7AL, UK

<sup>b</sup>Biome Bioplastics Ltd, Marchwood, Southampton, UK

### Supporting Information

Figure S1. LCMS analysis of authentic 2,4-pyridinedicarboxylic acid

Figure S2. LCMS analysis of samples of *R. jostii* pTipQC2-ligAB and wild-type *R. jostii* RHA1 grown on minimal media containing vanillic acid

Figure S3. LC-MS analysis of samples of *R. jostii* pTipQC2-ligAB grown on minimal media containing wheat straw lignocellulose

Figure S4. Growth curve for *R. jostii* pTipQC2-ligAB grown in 2.5L bioreactor.

Figure S5. Elution of 2,4-pyridinedicarboxylic acid from Amberlite IRA900 ion exchange

Figure S6. C18 Reverse phase HPLC analysis of 2,4-PDCA from bioreactor fermentation, after ion exchange purification

Figure S7. LCMS analysis of authentic 2,5-pyridinedicarboxylic acid

Figure S8. LCMS analysis of samples of *R. jostii* pTipQC2-praA and wild-type *R. jostii* RHA1 grown on minimal media containing vanillic acid

Figure S9. LC-MS analysis of samples of *R. jostii* pTipQC2-praA grown on minimal media containing wheat straw lignocellulose

Figure S10. Elution of 2,5-pyridinedicarboxylic acid from Amberlite IRA900 ion exchange

Figure S11. C18 Reverse phase HPLC analysis of 2,5-PDCA from bioreactor fermentation, after ion exchange purification

Figure S1. LCMS analysis of authentic 2,4-pyridinedicarboxylic acid

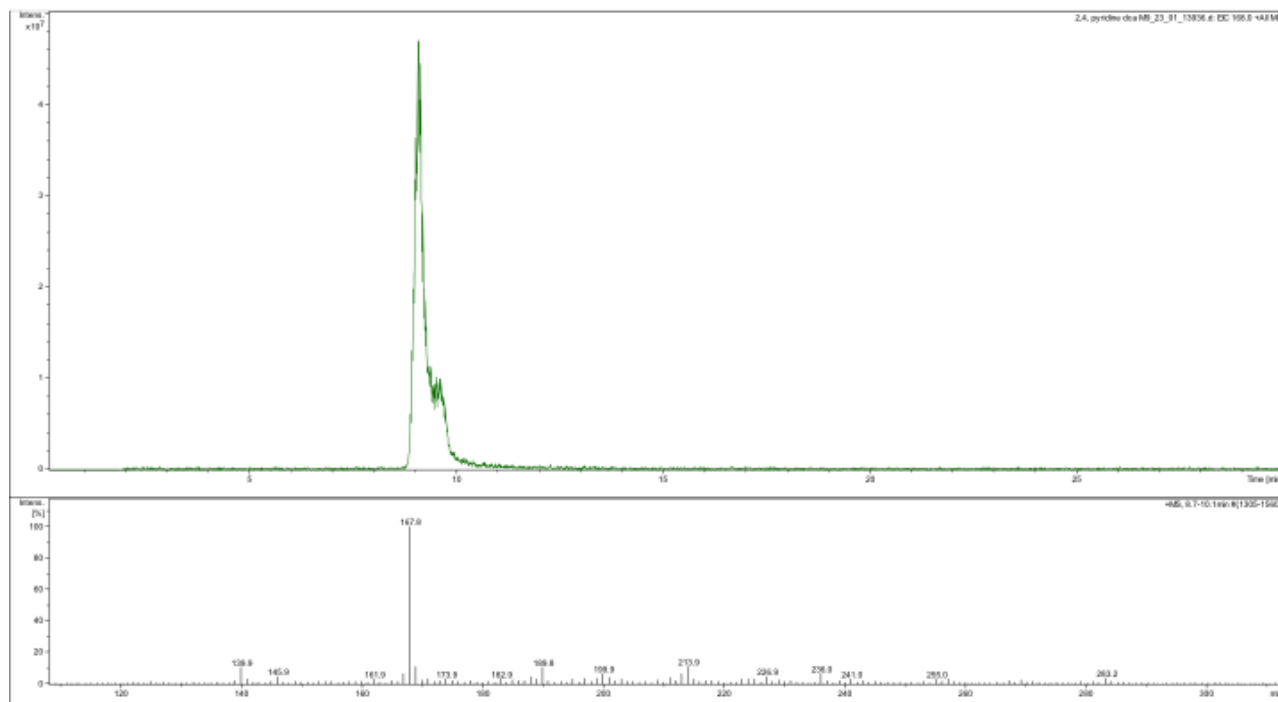


Figure S2. LCMS analysis of samples of *R. jostii* pTipQC2-ligAB and wild-type *R. jostii* RHA1 grown on minimal media containing vanillic acid (extracted ion chromatogram m/z 168.0)

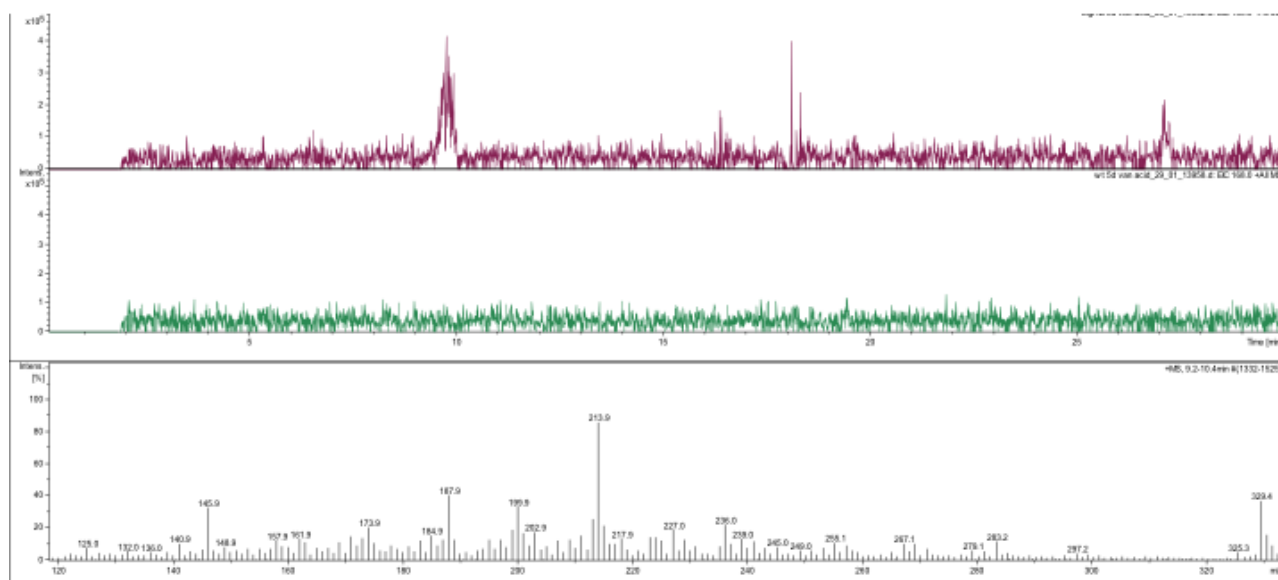


Figure S3. LC-MS analysis of samples of *R. jostii* pTipQC2-ligAB grown on minimal media containing wheat straw lignocellulose, after 5 days fermentation (extracted ion chromatogram m/z 168.0)

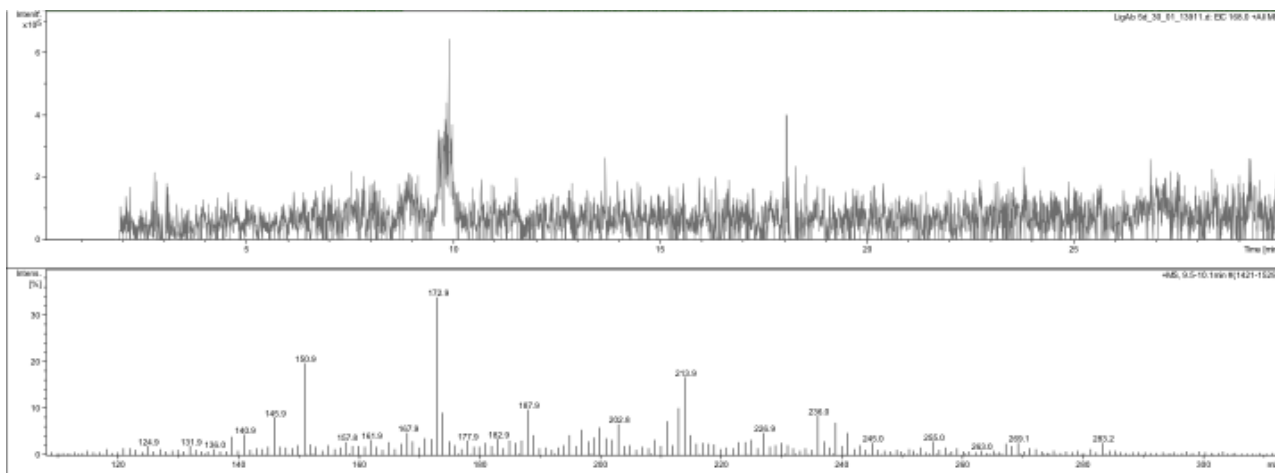


Figure S4. Growth curve (OD600, blue diamonds) for *R. jostii* pTipQC2-ligAB grown on M9 minimal media containing 1% wheat straw lignocellulose in 2.5L bioreactor. Relative yields of 2,4-PDCA bioproduct shown in red squares.

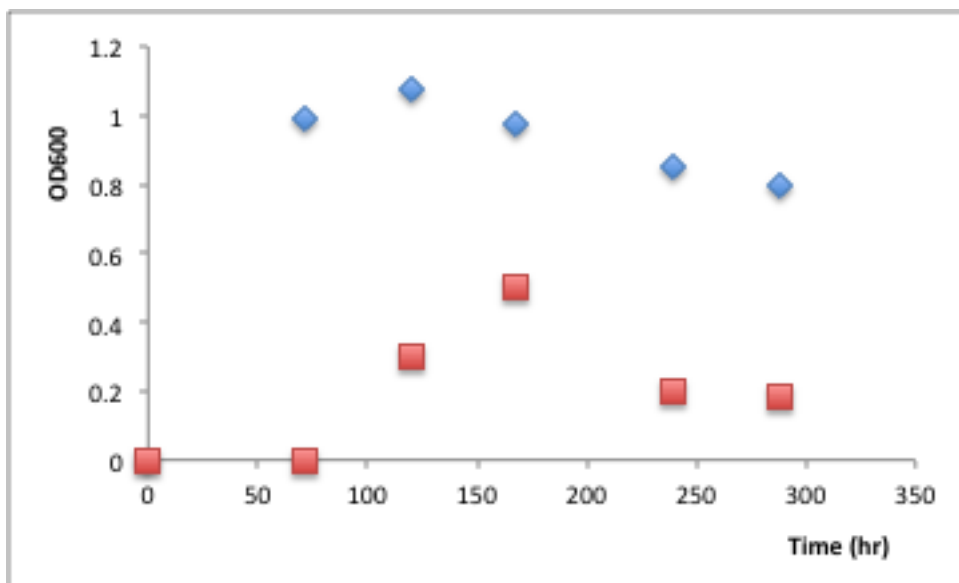


Figure S5. Elution of 2,4-pyridinedicarboxylic acid from Amberlite IRA900 ion exchange column, showing UV-vis spectrum of each eluted fraction, compared with authentic 2,4-PDCA (in red).

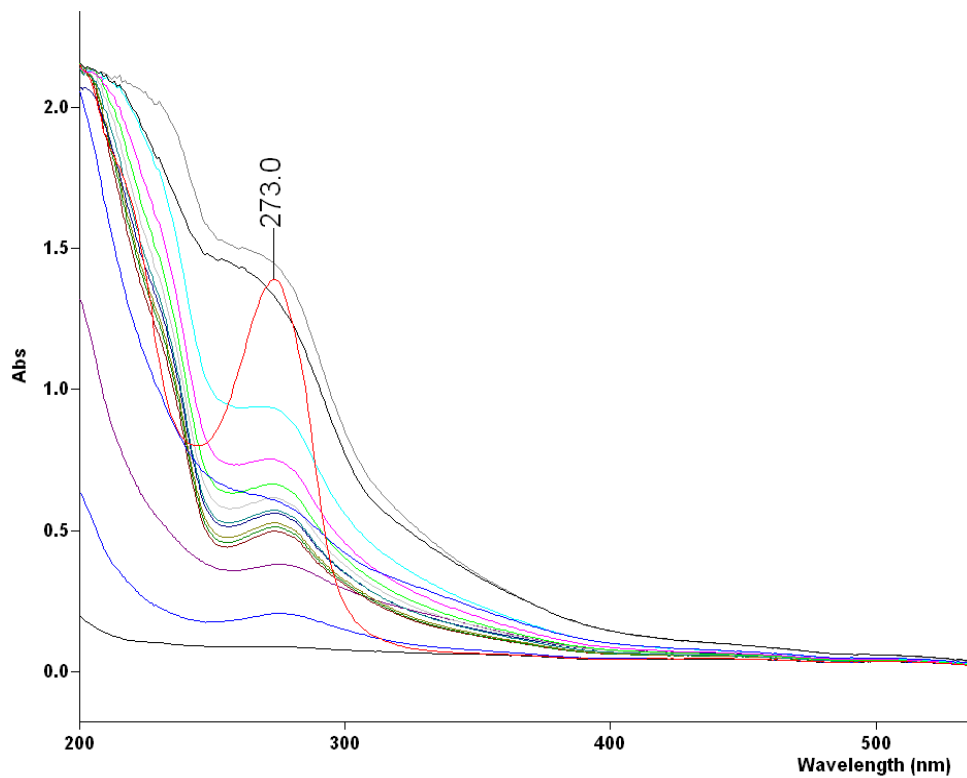


Figure S6. C18 Reverse phase HPLC analysis of 2,4-PDCA from bioreactor fermentation, after ion exchange purification

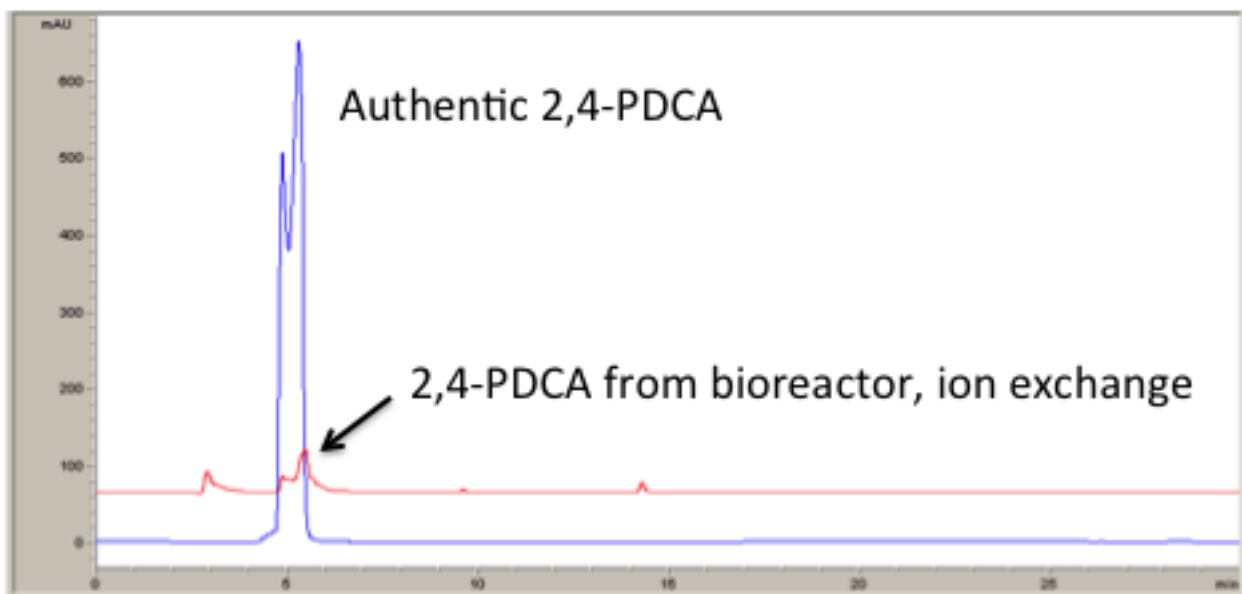


Figure S7. LC-MS analysis of authentic 2,5-pyridinedicarboxylic acid

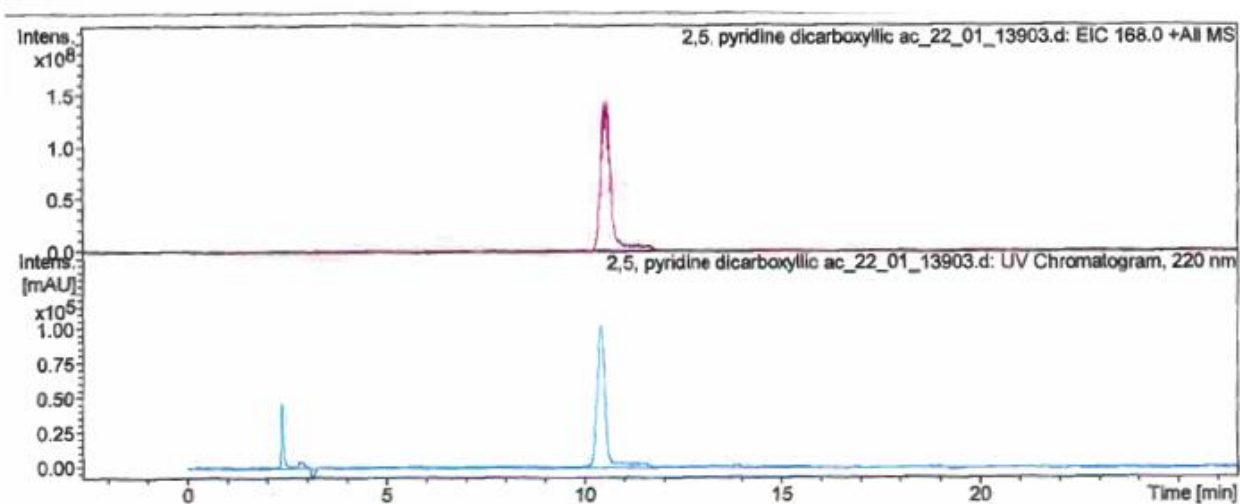


Figure S8. LC-MS analysis of sample of *R. jostii* pTipQC2-praA grown on minimal media containing vanillic acid (extracted ion chromatogram m/z 168.0)

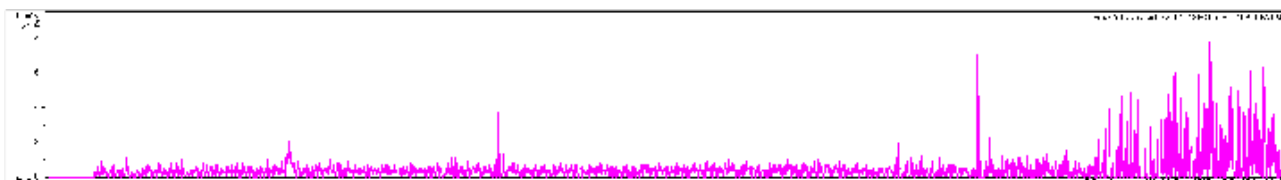


Figure S9. LC-MS analysis of sample of *R. jostii* pTipQC2-praA grown on minimal media containing wheat straw lignocellulose (extracted ion chromatogram m/z 168.0)

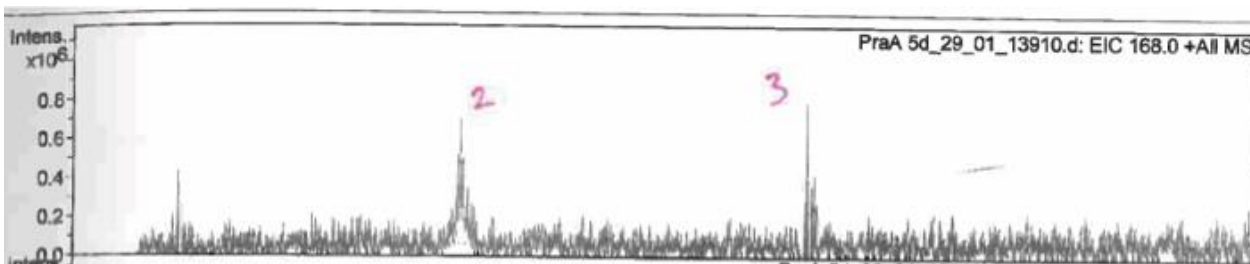


Figure S10. Elution of 2,5-pyridinedicarboxylic acid from Amberlite IRA900 ion exchange column, showing UV-vis spectrum of each eluted fraction, compared with authentic 2,5-PDCA (in red).

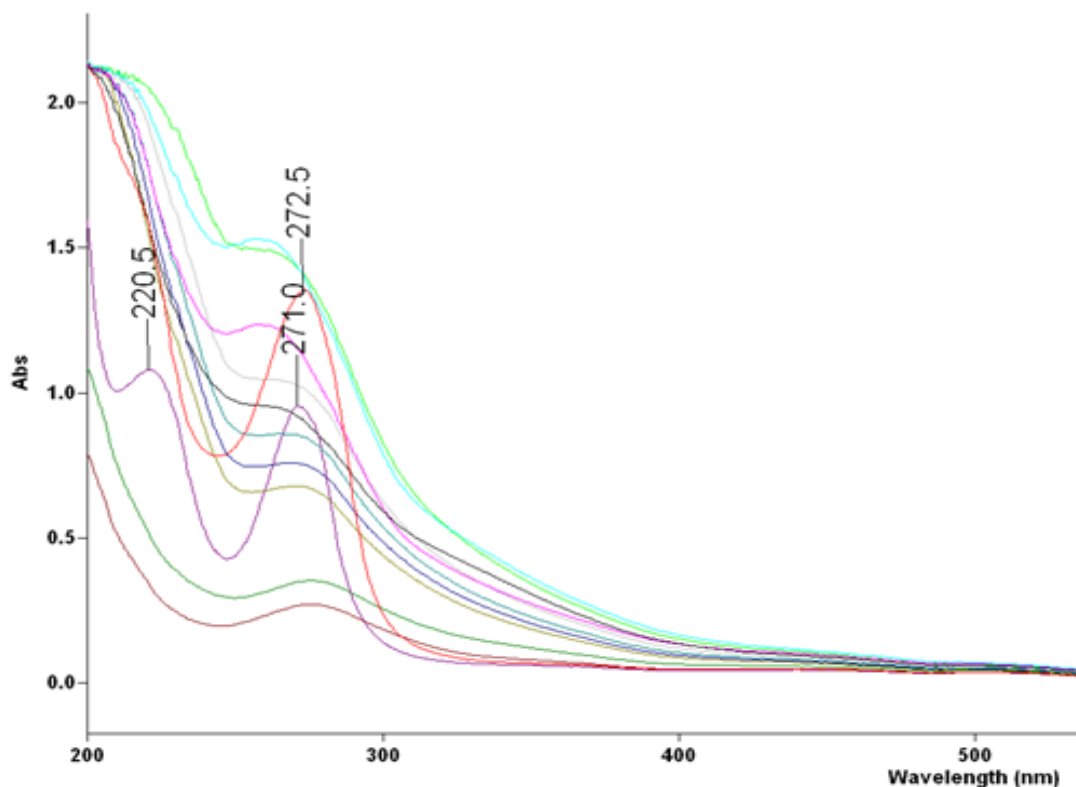


Figure S11. C18 reverse phase HPLC analysis of 2,5-pyridinedicarboxylic acid from bioreactor run, after ion exchange purification

